Department of Pharmacy, School of Pharmacy, University of Oslo, Norway

Influence of aqueous media properties on aggregation and solubility of four structurally related *meso*-porphyrin photosensitizers evaluated by spectrophotometric measurements

J. Sobczyński, H. H. Tønnesen, S. Kristensen

Received June 25, 2012, accepted August 25, 2012

Jan Sobczyński, Department of Pharmacy, School of Pharmacy, University of Oslo, P.O. Box 1068 Blindern, N-0316 Oslo, Norway
jan.sobczynski@farmasi.uio.no

Pharmazie 68: 100–109 (2013) *doi: 10.1691/ph.2013.2130*

Porphyrin photosensitizers tend to aggregate in aqueous solutions even in the micromolar concentration range. This is a challenge during formulation of e.g., parenteral preparations for photodynamic cancer therapy, or preparations for local or topical administration in antimicrobial photodynamic therapy. Monomerization is essential to achieve biocompatible drug formulations of high bioavailability and physiological response (i.e., photoreactivity) and low toxicity. The aggregation and solubilization of four structurally related *meso*-tetraphenyl porphyrin photosensitizers with nonionic (4-hydroxy), anionic (4-sulphonate; 4-carboxy) and cationic (4-trimethylanilinium) substituents were evaluated in various vehicles by use of UV-Vis spectroscopy. Substituents, overall charge and charge distribution influenced the pKa-values and interaction of the porphyrins with different solvents, excipients and impurities. Modification of medium polarity and solubilization by the nonionic surfactant Tween® 80 adjusted the acid-base equilibria and increased the solubility by reduction of porphyrin aggregation. The selected porphyrins were sensitive towards ionic strength, temperature and inorganic impurities to various extents. The results will be further used during development of parenteral and topical formulations of porphyrin photosensitizers for use in photodynamic therapy of cancer and bacterial infections.

1. Introduction

Photodynamic therapy (PDT) is a treatment modality used for some solid tumors and bacterial infections (Eszter-Borbas 2008). It involves three key components: a photosensitizer, light of appropriate wavelength and tissue oxygen. Light is absorbed by the photosensitizer, which becomes energetically activated, causing oxygen-mediated damage to the light-exposed tissues by the formation of Reactive Oxygen Species (ROS). The perfect photosensitizer should efficiently absorb red light, which permeates tissues (Eszter-Borbas 2008), or blue light for superficial antimicrobial PDT (Cormick et al. 2009). Additionally, it should effectively generate the first excited triplet state at sufficient energetic level and lifetime to produce singlet oxygen ($^1O_2$) by energy transfer to molecular oxygen. In order to enable a safe treatment, the photosensitizer has to be nontoxic in the absence of light, and ought to selectively accumulate in targeted tissues and be rapidly excreted from the body. It should also be chemically and photochemically stable, and easy to synthetize with high purity (Eszter-Borbas 2008). The search for such compounds focuses on porphyrin derivatives (O'Connor et al. 2009). The conjugated porphine ring system results in advantageous light absorption properties, but at the same time gives the molecules a lipophilic character (Eszter-Borbas 2008). As a result, many porphyrins are characterized by poor water solubility and a tendency to aggregate in aqueous environments (Moreira et al. 2008).

Low solubility and extensive aggregation are great hinders for bioavailability of several porphyrin photosensitizers, and a challenge to proper drug formulation (Moreira et al. 2008). Problems connected to aggregation include reduced photosensitization, increased uptake by the Mononuclear Phagocytic System (MPS), reduced uptake by target cells and increased risk of anaphylactic reactions (Hamblin et al. 2003; Mojzisova et al. 2007; Torchilin 2007). Cellular localization of porphyrin monomers and dimers will differ as demonstrated *in vitro* in Vero and RR 1022 cell lines (Seidlitz et al. 1990). Pharmaceutical technology can be used to overcome aggregation and low solubility, as well as to improve biological activity (Hamblin et al. 2003).

The absorption spectrum of most tetraphenyl porphyrins as monomeric free bases (i.e., the central porphine ring is uncharged) is characterized by the presence of four distinguishable Q-bands absorbing light $\geq$ 500 nm, representing the lowest $\pi \rightarrow \pi^*$ transition. The second $\pi \rightarrow \pi^*$ transition results in a single, intense, narrow band at around 400 nm called the Soret band.

Abbreviations: cmc - critical micelle concentration, ε - molar absorptivity coefficient, FWHM - full width at half maximum, i.v. - intravenous; log D - distribution coefficient, μ - ionic strength, MPS - Mononuclear Phagocytic System, $^1O_2$ - singlet oxygen, PDT - photodynamic therapy, RSD - relative standard deviation, pKa - acidity constant, pKa' - inflection point, ROS - Reactive Oxygen Species, TAPP - 5,10,15,20-Tetrakis(4-trimethylaniliniumphenyl) porphine, TCPP - 5,10,15,20-tetrakis(4-carboxyphenyl) porphine, THPP - 5,10,15,20-Tetrakis(4-hydroxyphenyl) porphine, TSPP - 5,10,15,20-Tetrakis(4-sulphonatophenyl) porphine.

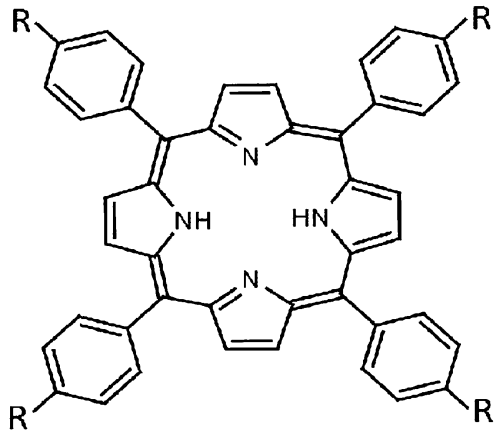

Protonated substituents	Protonated core	Free base	Deprotonated free base	Substituents (R)
	$TAPP^{4+}H_2^{2+}$ ⇄ (+ 2 H⁺) $TAPP^{4+}$; pKa' = 3.6, pKa = 2.3			$-N(CH_3)_3^+$
	$THPPH_2^{2+}$ ⇄ (+ 2 H⁺) THPP; pKa_1 ~ 4.5**	THPP ⇄ (- 4 H⁺) $THPP^{4-}$; pKa_2'=10.7, pKa_2=10.8		- OH
$TSPPH_2^{2+}$ ⇄ (+ 4 H⁺); pKa_1 < 1.0*	$TSPP^{4-}H_2^{2+}$ ⇄ (+ 2 H⁺) $TSPP^{4-}$; pKa_2'= 4.6, pKa_2= 5.2	$TSPP^{4-}$		$-SO_2OH$
$TCPPH_2^{2+}$ ⇄ (+ 4 H⁺); pKa_1 ~ 4.2*	$TCPP^{4-}H_2^{2+}$ ⇄ (+ 2 H⁺) $TCPP^{4-}$; pKa_2'= 6.0, pKa_2= 6.6	$TCPP^{4-}$		- COOH

Fig. 1: Molecular structure and ionic equilibria of the selected *meso*-porphyrins. The free base contains an uncharged central porphine ring. pKa' values (experimentally determined inflection points) and pKa values (acidity constants) were calculated as described in Section 2.6. *pKa_1 for TCPP and TSPP are taken from McMurry (2000) and Guthrie (1978), and Pasternack et al. (1972), respectively. **pKa_1 for THPP is based upon calculations performed by use of MarvinView computer software, Hungary

This band often shows a weaker blue-shifted shoulder, corresponding to n→π transition (Gouterman 1978). The absorption spectrum of protonated porphyrin diacids tends to consist of only two Q-bands, because the molecule symmetry changes by protonation of the porphyrin core (Janson et al. 1979). Protonation of anionic porphyrins in aqueous media has been shown to cause a red shift of the Soret band as well as a red shift and an increase in molar absorptivity (ε) of the far red Q-band (Maiti et al. 1995). Porphyrin dimerization is well described for anionic porphyrins. Monomers and dimers absorb light at similar wavelengths but with different molar absorptivities (Pasternack et al. 1972), as the dimers yield a slightly broadened Soret band with a reduced absorbance compared to monomeric units (Kano et al. 1990). Dimerization has been shown to be hindered by addition of ethylene glycol (Pasternack et al. 1972). Porphyrin aggregates have been observed as broad blue shifted bands (H-aggregates) or narrow red-shifted bands (J-aggregates), i.e. in the 450–500 nm region (Li et al. 2007). J-Aggregates are described as horizontally displaced parallel planes of porphyrin, because of edge-to-edge stacking. H-aggregates constitute stacked planes of porphyrin resulting from face-to-face aggregation (Maiti et al. 1998). Different factors have been shown to influence aggregation, including increased porphyrin concentration (Pasternack et al. 1972), acidification and reduced polarity of the environment (Choi et al. 2003), metal ions (Ma et al. 2008) and ionic and nonionic surfactants (Maiti et al. 1998).

Four structurally related *meso*-tetraphenyl porphyrin photosensitizers were selected for the experiments, whose photodynamic activity against pathogenic microorganisms or cancer cell lines has been proven experimentally (Cormick et al. 2009; Oba 2007). The photosensitizers will serve as model compounds to study the interactions between photosensitizer and drug vehicle on a mechanistic level, and determine the impact of pharmaceutical formulation on photochemical reactivity. The aim of our study was to evaluate the influence of aqueous media properties (i.e., pH, ionic strength and temperature) and additives (i.e., cosolvent, surfactant, impurities) on aggregation and solubility of the selected porphyrins by use of spectroscopic measurements. Our study includes evaluation of pKa values, which influence aggregation and solubility. The obtained knowledge will serve as a background for further development of parenteral and topical formulations of porphyrin photosensitizers for use in PDT of cancer.

2. Investigations, results and discussions

2.1. Molecular properties of selected meso-porphyrins

The selected photosensitizers represent the *meso*-tetrakis phenyl substituted series of porphyrins. This class of compounds comprises the porphine ring, which is substituted at the 5,10,15 and 20 positions (Fig. 1). The neutral p-hydroxyphenyl porphyrin (THPP), the cationic trimethylaniliniumphenyl porphyrin (TAPP), and the anionic carboxyphenyl porphyrin (TCPP) and sulphonatophenyl porphyrin (TSPP) were selected as model compounds. The molecules are symmetrical, and none of them possess spatial isomers. Representative, predicted 3-D

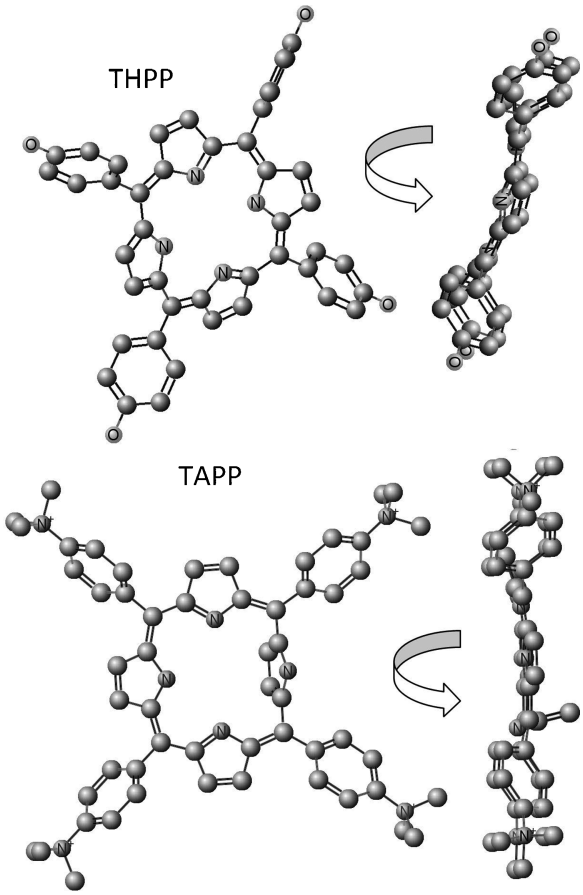

Fig. 2: 3-D Structures of THPP (above) and TAPP (below), generated by the MarvinView computer software, Hungary. The figure presents the structures from different angles

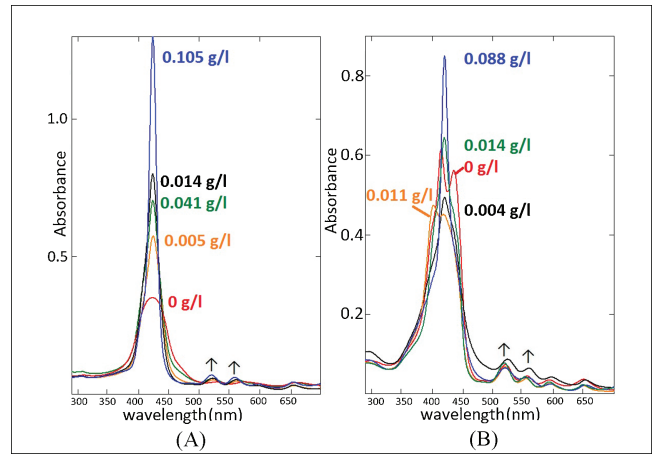

Fig. 3: UV-Visible absorption spectra of 5 μM THPP (A) and TCPP (B) as a function of Tween® 80 concentration in aqueous solution. Arrows indicate trends in absorbance upon increasing Tween® 80 concentration

structures of THPP and TAPP are presented in Fig. 2. THPP and TCPP show a saddle-like 3-D structure. The central ring of TAPP and TSPP has only one pyrrole ring orthogonal to the main plane of the porphyrin. The in silico method (MarvinView software, Hungary) holds limitations, as the estimated structure of TSPP is not consistent with the previously proposed model confirmed by NMR studies (Choi et al. 2003).

Different ligands present in p-position of the phenyl groups influence physicochemical properties of the compounds. Sulfonic, carboxylic and trimethylanilinium groups have electron withdrawing effects while hydroxyl groups exhibit strong electron-donating properties (McMurry 2000). The peripheral charge localization is strongest for -$N(Me)_3^+$ (permanent cation), followed by -SO_3H (strong acid) and -COOH (weak acid) (McMurry 2000). In this study, only protonation of the imino (-N =) nitrogens was investigated, because deprotonation of the pyrrole (-NH-) nitrogens is assumed to occur only in highly alkaline environment, i.e., pH > 14 (Cunderlikova et al. 2001) and the effective basic centres are limited to the two imino nitrogens when considering steric, electrostatic and resonance energy (Phillips 1960). As a result, TAPP is positively charged regardless of environment. The three other compounds possess four acidic substituents in addition to the two basic imino groups (Fig. 1). As the pKa-value of the sulphonic groups in TSPP is reported to be ≤ 1 (Pasternack et al. 1972; Guthrie 1978), the TSPP dication will hardly exist under normal aqueous conditions. Benzoic acid has pKa = 4.2 (McMurry 2000). We predict about the same value as representative for the carboxylic groups of TCPP, which can then exist also as a dication. The other pKa values were determined as described in Section 2.6, and presented in Fig. 1.

Charge changes of the selected compounds are reflected in the distribution coefficients (logD values) within pH scale (0–14) as calculated by use of MarvinView software, Hungary. The software does not enable introduction of experimentally obtained pKa values, and the calculated logD values are considered approximate. The hydrophilic TSPP and TAPP (logD = –1.6 and –4.5 at pH 7, respectively) (Fig. 1) dissolve well in water, while the lipophilic neutral THPP (logD = 10.0 at pH 7) is only slightly soluble in water. Changes in pH towards acidic or alkaline conditions result in increased solubility of THPP by introduction of charge. There is a marked difference in lipophilicity between the positively charged cation (logD = 7.2 at pH 4) and the negatively charged anion of TCPP (logD = –3.8 at pH 8). All the compounds are soluble in methanol, which creates convenient conditions for the apolar macromolecular ring of porphyrin compounds, thus stock solutions were prepared in this solvent. However, polarity of the medium can influence the position of the bands in the absorption spectrum of porphyrins (Manna et al. 1995).

Overall charge and its localization influence aggregation of the porphyrins. TCPP and TSPP have zwitterionic nature that enables intermolecular attractions between the negative charges of the peripheral groups and the positively charged porphyrin cores. The saddle conformation of TCPP may further increase aggregation of this compound, as the distance between oppositely charged groups is reduced (Choi et al. 2003). Zwitterionic porphyrins which form dimers and aggregates are however, expected not to stack in their free base form due to electrostatic repulsion forces. Nevertheless, dimerization of TCPP free base was observed as deviation from linear absorptivity above 10^{-5} M by Pasternack et al. (1972). Overall porphyrin charge, its localization and electronic density in the porphyrin core have also been shown to be very important for porphyrin interactions with both ionic and nonionic surfactants (Maiti et al. 1998). These phenomena have been observed as increased/decreased molar absorptivity (ε) of bands ascribed to monomers and different aggregates, and shifts of these bands in the UV-Vis absorption spectra. Kadish et al. (1989) have shown that negligible shifts reflect minor levels of interactions between TSPP porphyrins with charged and uncharged surfactants, while significant shifts mark strong porphyrin-surfactant interactions.

2.2. Absorption properties of THPP

The absorption spectrum of THPP is highly dependent on solvent properties. THPP is only slightly soluble in water, which is reflected by the reduction in ε as the concentration of THPP is increased in aqueous solution (Table). pH of 5 μM THPP aque-

Table: Absorption maxima (nm) of THPP; TAPP; TSPP; and TCCP at 0.5 and 5 μM

Compound	Absorption maximum (nm) ($\varepsilon \bullet 10^5$ M^{-1} cm^{-1})					
THPP	0.5 μM	5 μM		Q bands (nm)		
EMSURE® water	416 (1.54; RSD = 3.9%)	416 (1.05; RSD = 5.5%)	529	578		664
Methanol	418 (4.80; RSD = 2.0%)	418 (4.56; RSD = 3.0%)	517	555	591	649
Tween 80® > cmc	424 (3.83; RSD = 5.1%)	424 (3.39; RSD = 6.2%)	520	558	597	655
Tap water	415 (1.56; RSD = 9.7%)	415 (1.00; RSD = 4.2%)	530	573		660
EMSURE® water with equimolar Fe^{3+}	414 (0.31; RSD = 19.2%)	414 (1.07; RSD = 3.6%)	529			669
EMSURE® water (37 °C)	416 (1.61; RSD = 3.2%)	416 (1.19; RSD = 4.4%)	530	574		660
EMSURE® water with 0.1 M NaCl	416 (1.49; RSD = 8.4%)	416 (0.65; RSD = 15.5%)	528	575		663
TAPP	0.5 μM	5 μM		Q bands (nm)		
EMSURE® water	412 (3.93; RSD = 2.8%)	412 (3.61; RSD = 2.0%)	514	550	579	633
Methanol	413 (3.62; RSD = 6.1%)	413 (3.53; RSD = 1.8%)	511	544	586	645
Tween 80® > cmc	413 (3.74; RSD = 5.6%)	413 (3.68; RSD = 2.7%)	515	551	580	635
Tap water	412 (3.51; RSD = 9.9%)	412 (3.38; RSD = 0.8%)		539	576	
EMSURE® water with equimolar Fe^{3+}	412 (3.99; RSD = 8.4%)	412 (3.82; RSD = 3.6%)	515	550	580	633
EMSURE® water (37 °C)	412 (3.55; RSD = 6.0%)	412 (3.76; RSD = 1.1%)	515	551	579	634
EMSURE® water with 0.1 M NaCl	412 (3.55; RSD = 5.0%)	412 (3.77; RSD = 0.8%)	514	551	579	633
TSPP	0.5 μM	5 μM		Q bands (nm)		
EMSURE® water	414 (3.49; RSD = 3.5%)	414 (1.71; RSD = 12.7%)	516	553	595	644
	434 (0.73; RSD = 7.2%)	434 (2.24; RSD = 10.3%)				
Methanol	415 (4.32; RSD = 3.3%)	415 (4.31; RSD = 3.4%)	512	547	589	644
Tween 80® > cmc	419 (4.08; RSD = 0.8%)	419 (3.99; RSD = 0.9%)	515	550	590	644
Tap water	413 (4.39; RSD = 7.4%)	413 (3.88; RSD = 3.4%)	517	539	579	634
EMSURE® water with equimolar Fe^{3+}	414 (3.16; RSD = 3.8%)	414 (1.07; RSD = 5.0%)	518	556	596	645
	434 (0.96; RSD = 13.1%)	434 (3.04; RSD = 3.7%)				
	488 (0.09; RSD = 39.1%)	489 (0.05; RSD = 3.8%)				
EMSURE® water (37 °C)	414 (4.08; RSD = 2.5%)	414 (2.71; RSD = 13.3%)	516	553	586	644
	434 (0.32; RSD = 10.1%)	434 (2.00; RSD = 1.0%)				
EMSURE® water with 0.1 M NaCl	414 (4.45; RSD = 3.0%)	414 (2.97; RSD = 2.3%)	516	553	583	642
	434 (0.25; RSD = 18.3%)	434 (0.75; RSD = 9.5%)				
TCPP	0.5 μM	5 μM		Q bands (nm)		
EMSURE® water	416 (1.80; RSD = 6.8%)	416 (1.38; RSD = 4.7%)	521	557	594	650
	436 (1.06; RSD = 5.0%)	436 (1.33; RSD = 4.7%)				
Methanol	415 (3.70; RSD = 5.3%)	415 (4.38; RSD = 0.3%)	513	547	589	646
Tween 80® > cmc	421 (3.16; RSD = 9.5%)	421 (3.14; RSD = 6.4%)	516	549	591	648
Tap water	414 (3.62; RSD = 7.3%)	414 (3.26; RSD = 0.4%)	519	552	578	636
EMSURE® water with equimolar Fe^{3+}	416 (0.91; RSD = 12.8%)	403 (0.94; RSD = 0.5%)	523	558	593	650
	436 (0.67; RSD = 15.4%)	416 (1.02; RSD = 1.9%)				
		436 (0.94; RSD = 2.0%)				
EMSURE® water (37 °C)	416 (4.14; RSD = 23.5%)	416 (1.47; RSD = 3.4%)	521	557	593	650
	438 (0.46; RSD = 12.2%)	438 (1.19; RSD = 8.3%)				
EMSURE® water with 0.1 M l NaCl	416 (2.30; RSD = 17.5%)	416 (1.46; RSD = 2.7%)	522	557	593	650
		438 (0.90; RSD = 5.5%)				

Spectra were analyzed under different conditions (ambient temperature when not stated otherwise). Molar absorptivity ($\varepsilon \bullet 10^5$ M^{-1} cm^{-1}) has been calculated for the main bands in the 400–500 region ($n \geq 5$). Concentration of Tween® 80 = 1 g/l. For pH of the aqueous samples: confer the text.

ous solution is 6.58 (n = 5, RSD = 0.8%), thus THPP is likely present mainly as the free base. The Soret band (416 nm) is broad (FWHM = 48 nm, RSD = 5.8%, n = 5) with a small shoulder at 475 nm (Fig. 3A). Three Q-bands can be distinguished in the spectrum (Table). Broadening of the Soret band likely means there are coexisting absorbing species. It can be various aggregates, as the lipophilic THPP is likely to form associates by stacking in polar solvent.

Titration with hydrochloric acid leads to decreased absorbance at the Soret band. Below pH 4.3 the absorptivity of the Soret band increases again, presumably caused by increased solubility due to protonation of the imino nitrogens of the core. A new band arises at 322 nm, and the red Q-band (664 nm) is broadened and bathochromically shifted to 690 nm (Fig. 4A). Manna et al. (1995) reported a similar strong Q-band at 702 nm upon titration of THPP in dimethylformamide with hydrochloric acid. The red Q-band seems to be characteristic for the protonated porphyrin core, since it appears for all four compounds at low pH (Figs. 4A-D). The red Q-band of THPP is bathochromically shifted in acidic aqueous solution when compared to the corresponding bands of the other porphyrins investigated (690 nm vs. 640–661 nm, see Section 2.3–2.5), which might be caused by the electron transfer from the -OH substituents of THPP towards the core (positive resonance effect). An increase of pH from neutral to alkaline pH and formation of THPP anion(s) increases the solubility and hence the molar absorptivity of the Soret band, which becomes red shifted towards 438 nm. There is a corresponding increase in one of the Q-bands (594 nm) by an increase in pH.

The absorption spectrum of THPP in methanol is characterized by a narrow Soret band (FWHM = 14 nm, RSD = 4.2%, n = 3) with highly increased molar absorptivity and four distinct Q-bands (Table). These changes compared to aqueous solution are characteristic for monomeric free base porphyrins (see Section 1). Absorbance of THPP in aqueous solution at 416 nm as a function of methanol concentration is presented in Fig. 5A. A steep increase in absorbance at methanol con-

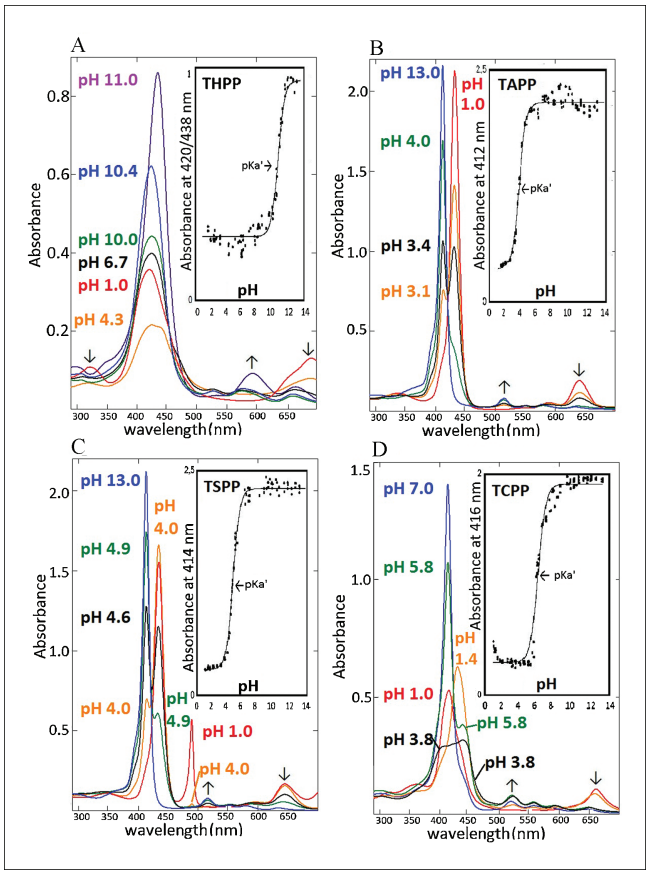

Fig. 4: UV-Visible absorption spectra of THPP (A); TAPP (B); TSPP (C); and TCPP (D) at 5 μM, respectively, during aqueous pH-titration. Arrows indicate trends in absorbance upon increasing pH. Inset: Curve fitting for absorbance at the respective absorption maximum as a function of pH. The data are given by circles, while the solid line is the fitted curve; $\chi^2 = 0.16$ (THPP); 0.53 (TAPP); 0.44 (TSPP); and 0.81 (TCPP). Calculated inflection points at $\mu = 0.1$ M are pKa' = 10.7 (THPP); 3.6 (TAPP); 4.6 (TSPP); and 6.0 (TCPP)

tent > 30% shows solubilization of THPP, further indicated by narrowing of the Soret band. The absorptivity is then linearly increased ($R^2 = 0.994$) as a function of methanol content in the range 40–80%, reaching a plateau at ≥ 80% methanol where optimal solubilization and monomerization seem to be achieved. Changes in absorptivity and narrowing of the Soret band is accompanied by blue shifts of the Q-bands (Table).

Absorbance at the Soret band maximum vs. Tween® 80 concentration is presented in Fig. 5B. An increase in molar absorptivity of the Soret band was observed even at Tween concentrations below the critical micelle concentration; cmc (Fig. 3A; cmc = 0.014 g/l, as determined by Wan et al. 1974). This indicates that interactions between porphyrin and surfactant unimers take place prior to micellization (Kadish et al. 1990). At cmc the absorbance vs. Tween® 80 concentration curve reaches a small plateau, and the Soret band acquires the shape typical for monomers. The absorption spectrum of THPP in presence of Tween® 80 > cmc (Fig. 3A) resembles the spectrum observed in methanol, with a narrowed Soret band (FWHM = 13.5 nm, RSD = 0%, n = 5 at Tween 80® concentration 1 g/l) which is red-shifted (424 nm) when compared to pure aqueous solution, and four distinct Q-bands (Table). This indicates solubilization of THPP. Addition of the neutral surfactant Triton X-100 has previously resulted in similar observations (Li et al. 2007).

Addition of sodium chloride (0.1 M) caused a substantial decrease in ε of the Soret band at 5 μM THPP concentration (Table), likely due to salting out of the lipophilic compound. A rise in temperature (to 37 °C) slightly increased the solubility at the highest concentration of THPP (Table). Addition of ferric ions at equimolar THPP/Fe^{3+} concentrations = 5 μM resulted in removal of one of the Q-bands. There was a substantial decrease in the Soret band absorptivity upon addition of 0.5 μM ferric ions to 0.5 μM THPP aqueous solution, which resulted in a high RSD (Table). These results indicate complexation of Fe^{3+} with the porphyrin core, as expected from the strong positive resonance effect of THPP. However, the absorption properties of THPP were not sensitive to the water quality.

2.3. *Absorption properties of TAPP*

TAPP (5 μM) dissolved in EMSURE® water gives a pH = 6.55 (n = 5; RSD = 1.4%), i.e., TAPP is present as the free base (overall charge 4 +). The UV-Vis absorption spectrum of TAPP in water consists of a sharp Soret band at 412 nm (FWHM = 12.5 nm, RSD = 3.6%, n = 5) and four Q-bands in the range 514 nm to 633 nm (Table), which is characteristic for the free base monomer, as previously described. During pH titration, no aggregation of TAPP was observed by spectrophotometric evaluation, which is as expected due to the permanent positive charge and consequent electrostatic intermolecular repulsion. Upon a change in the pH from neutral to acidic, a new band arises at 432 nm, reducing the band at 412 nm into a shoulder (Fig. 4B). The change in the molar absorptivity at these two wavelengths is inversely related and there is a clear isosbestic point at 420 nm, as expected for the simple equilibrium between TAPP acidic and free base forms (Fig. 1). In acidic aqueous solutions there are also two pronounced bands at 590 nm and 640 nm, representing the pattern characteristic for porphyrin diacidic monomers (Janson et al. 1979). In basic solution the Soret band decreases slightly (Fig. 4B, inset) and there is a slight increase of the shoulder at 393 nm (corresponding to n→π transition) but without changes of the Q-bands, compared to neutral conditions.

In methanol the molar absorptivity and position of the Soret band (FWHM = 14 nm, RSD = 0%, n = 5) is unchanged (413 nm) but the four Q-bands at 511 nm to 645 nm are shifted in relation to TAPP dissolved in water (Table), further indicating monomerization in aqueous solution and some influence of media properties (e.g., polarity) on the intramolecular electronic distribution. Addition of Tween 80® to aqueous solutions of TAPP does not influence the absorption properties (Table). It may then be assumed, that TAPP is not solubilized by Tween® 80 in aqueous solution, or only peripherally attached to the micelles, due to high hydrophilicity and as a result of peripheral charge localization in TAPP (Thompson 1980).

Addition of sodium chloride at moderate ionic strength (μ = 0.1 M) or ferric ions did not cause any changes in absorption properties (Table). However, the water quality did influence the absorption properties of the four Q-bands, which were removed or hypsochromically shifted (Table). Increasing the temperature to 37 °C did not cause any apparent changes in absorption properties, as expected due to high solubility and absence of aggregates (Table).

2.4. *Absorption properties of TSPP*

The absorption spectrum of TSPP in EMSURE® water (pH = 5.5 at 5 μM, n = 5, RSD = 3.5%) is characterized by the intense Soret band with maxima at 414 nm (representing the free base) and 434 nm (representing the zwitterion) and four Q-bands in the range 516 nm to 644 nm (Table). The RSD values are high due to the presence of two species in equilibrium at pH close to pKa_2 (see Section 2.6) at non-buffered conditions. The Soret band at 414 nm has a weak shoulder at 396 nm, corresponding to n→π transition of electrons in the core of the free base (Gouterman 1978). The equilibrium between the free base and the zwitte-

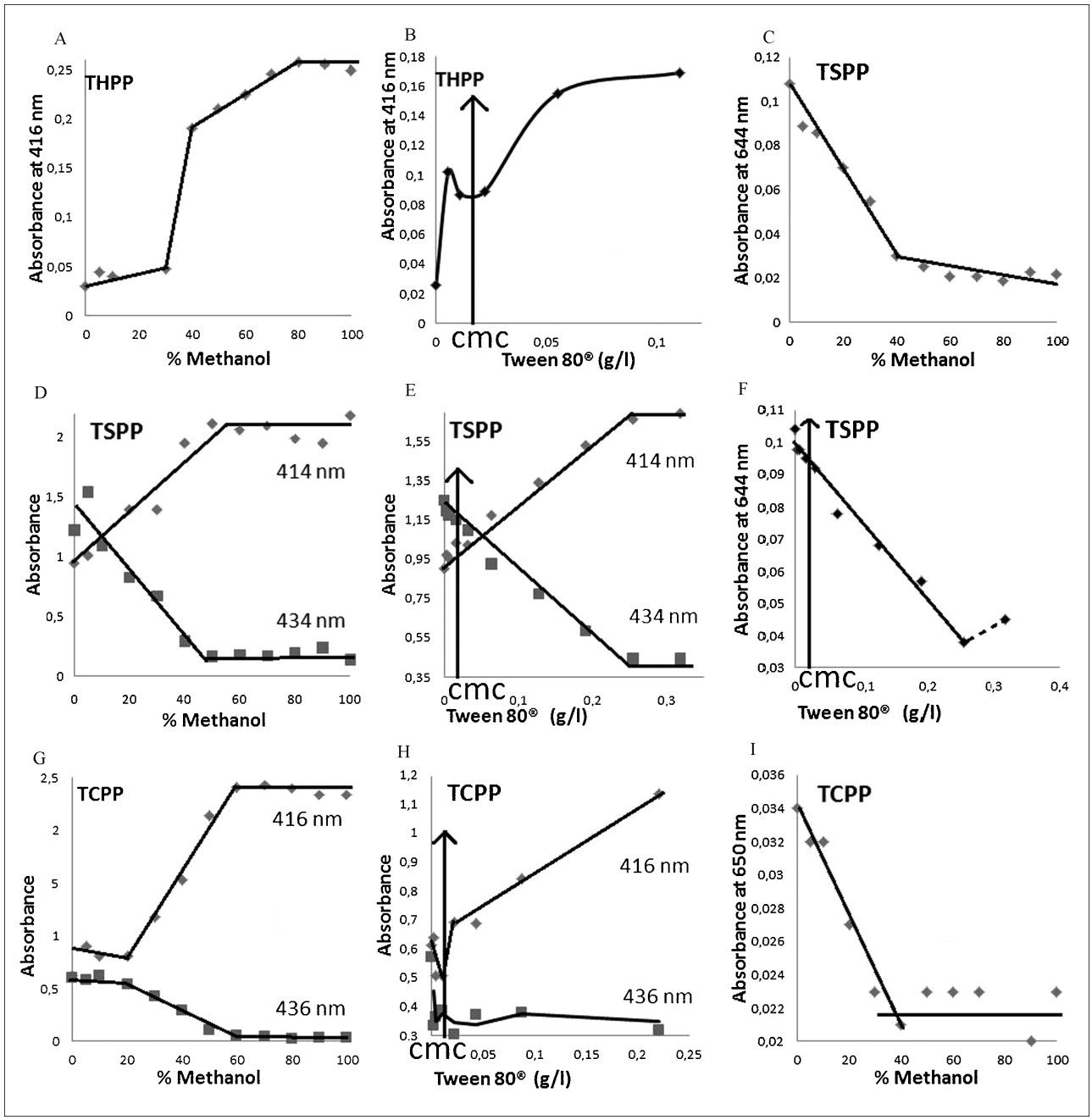

Fig. 5: Absorbance at selected wavelengths as a function of methanol content in binary water-methanol mixtures (A, C, D, G, I) or Tween® 80 concentration (B, E, F, H) for 0.6 μM THPP (A, B), 5 μM TSPP (C, D, E, F) and 5 μM TCPP (G, H, I). Each point is an average of ≥ 3 measurements; deviation ≤ 13.8%. The CMC of Tween® 80 (i.e. 0.014 g/l according to Wan et al. 1974) is indicated by an arrow

rion, evaluated by calculations of the relative molar absorptivity at 414 nm vs. 434 nm is dependent on the TSPP concentration within the μM range (Table). Correspondingly, ε at 644 nm, which is characteristic for the protonated porphyrin core, is lower at 0.5 μM (0.059×10^5 M^{-1} cm^{-1}; n = 5; RSD = 1.5%) than at 5 μM (0.19×10^5 M^{-1} cm^{-1}; n = 5; RSD = 0.9%). The shift of the equilibrium towards the zwitterion at the highest concentration of TSSP is likely a result of aggregation of the zwitterion, which is in accordance with previous studies (Ohno et al. 1993). Acidification leads to an increase of the band at 434 nm with a corresponding decrease of the band at 414 nm, and an increase of the band at 644 nm with a simultaneous red shift to 650 nm (Fig. 4C). The sharp band at 490 nm (FWHM = 8.5 nm, RSD = 0%, n = 3 at pH 1) present at pH ≤ 4.3 is previously reported to occur as a result of stacking into J-aggregates (Ohno et al. 1993). Formation of this peak is accompanied by a decrease in absorbance at 434 nm at pH < 2.5 (Fig. 4C), which is illustrating a gradual aggregation of the monomeric zwitterionic species. Conversion of monomeric TSPP zwitterions into J-aggregates has previously been shown to result in aggregates of different aggregation number, while dimers were not detectable (Maiti et al. 1995). At basic pH the spectrum consists of a narrow Soret band at 413 nm (FWHM = 13.5 nm, RSD = 2.2%, n = 3) with the characteristic shoulder at 394 nm and four Q-bands (Fig. 4C), following the pattern of free base monomeric porphyrins, as described in Section 1. The Q-band at 516 nm is growing characteristically with increasing pH.

The Soret band at 434 nm (zwitterion) is removed when TSPP is dissolved in methanol (Table), and there is a concomitant increase of the shoulder at 396 nm. Dimerization is not expected to occur at these conditions, as the concentration is too low (Corsini et al. 1986). The presence of only one species is reflected as a decrease in the RSD value (Table). The absorbance at selected wavelengths vs. methanol content is presented in

Fig. 5 C and 5 D. The absorbance of the red Q-band at 644 nm (zwitterion) shows a linear decrease ($R^2 = 0.978$) up to 40% MeOH, followed by a plateau (Fig. 5C). There is a linear increase in absorbance at 414 nm (free base) and a corresponding linear decrease at 434 nm (zwitterion) at increasing methanol content up to 40% ($R^2 = 0.914$ and 0.880, respectively; Fig. 5D). The slopes are similar (+ 0.023 vs.–0.027) confirming that the observed change is a one-to-one reaction. An increase in methanol content from 0 to 80% causes a decrease in pKa_2 of TSPP by 1.56 units (Farajtabar et al. 2010). The observed spectral changes are thus likely to be a result of a gradual change from the zwitterion into the free base form of TSPP. This transition also influences the Q-bands, as an increase of MeOH content results in a 4-Q-bands pattern, typical for the monomeric free base (see Section 1).

Addition of Tween® 80 leads to spectral changes similar to the addition of methanol, as presented in Fig. 5E and 5F. There is a linear increase in the absorbance at 414 nm ($R^2 = 0.987$) and a corresponding linear decrease at 434 nm ($R^2 = 0.985$) with similar slopes: (+ 2.9 vs. –3.1, respectively). At concentrations of Tween® 80 > 0.25 g/l the curves flatten out, and remain more or less unchanged up to 2.2 g/l (data not shown). The shoulder at 396 nm is increasing with increasing Tween® 80 concentration, and four Q-bands can be distinguished in aqueous TSPP solution enriched with Tween® 80 (Table), further indicating a switch from zwitterionic form to monomeric free base. The absorbance at the red Q-band is decreasing linearly with increasing Tween® 80 content up to 0.25 g/l ($R^2 = 0.939$; Fig. 5F), and occurs also at concentrations of Tween® 80 < cmc (i.e., < 0.014 g/l). Further, there are no observed spectral changes in the Soret band by changing the Tween® 80 concentration around cmc (data not shown). The changes in spectral properties by addition of Tween® 80 are probably caused by interactions with surfactant unimers and micellar surfaces rather than by solubilization of the porphyrin into the micelles. The nonionic surfactant, Triton X-100 has been shown to reduce the pKa_2-value of TSPP by more than 2.5 units (Papkovskii et al. 1989). It has been proposed, that TSPP free base can be present in the hydration layer of Triton X-100, constructed by the polyoxyethylene chains (Li et al. 2007). The interaction between free base of TSPP and neutral Tween® 80 molecules is probably facilitated by the absence of charges at the hydrophobic porphine ring. The equilibrium is shifted towards free base resulting in proportional increase of the band at 414 nm and decrease of the bands at 434 nm and 644 nm.

Addition of NaCl ($\mu = 0.1$ M) to an aqueous solution of 5 μM TSPP lowers the pH from 5.5 in pure water to 4.9 (n = 5, RSD = 0.4%). This is in accordance with the reduction in pKa_2 by an increase in μ (Fig. 1, outlined in Section 2.6), resulting in the observed transition from porphyrin zwitterion (434 nm) to free base (414 nm) (Table). Correspondingly, ε at 644 nm is reduced at $\mu = 0.1$ M (0.063×10^5 M^{-1} cm^{-1}; n = 5; RSD = 10.6%) compared to the respective value in pure water (0.192×10^5 M^{-1} cm^{-1}; n = 5; RSD = 0.9%). The apparent transition from porphyrin zwitterion (434 nm) to free base (414 nm) observed at elevated temperature (37 °C, Table) can also be ascribed to a decrease in the pKa_2-value, as a similar phenomenon has been reported for aromatic heterocyclic nitrogens (Ashton et al. 1982).

It was previously demonstrated that addition of divalent and trivalent metal ions decreases the Soret band absorption of TSPP and induces creation of J-aggregates (Ma et al. 2008). Addition of ferric nitrate to a TSPP solution at a concentration equimolar to the photosensitizer (0.5 or 5 μM) induced the formation of a new band at 489 nm, which has been reported to be characteristic for J-aggregates (Ohno et al. 1993). Simultanously, a decrease in the absorbance at 414 nm and a corresponding increase at 434 nm was observed (Table), as the equilibrium is switched from the free base towards a zwitterion by the interaction with the metal ion. The effect is less pronounced at low concentrations, where the RSD is high due to a low molar absorptivity (Table). Unexpectedly, the use of tap water as a solvent removed the 434 nm band in the absorption spectrum of TSPP. The absorptivity was correspondingly increased at 413 nm, and several Q-bands were blue shifted as compared to EMSURE® water (Table). Chemical purity of excipients will thus be essential during pharmaceutical formulation of TSPP.

2.5. Absorption properties of TCPP

The absorption spectrum of TCPP in EMSURE® water (at 5 μM pH = 6.4; n = 5; RSD = 3.7%) is characterized by the intense split Soret band with maxima at 416 and 436 nm, with a shoulder at 397 nm and four Q-bands at 521 nm to 650 nm (Fig. 3B; Table). In pure aqueous solution TCPP is present mainly as a free base (band at 416 nm) and a zwitterion (band at 436 nm). As for TSPP, the equilibrium between the free base and the zwitterion, evaluated by calculations of the relative molar absorptivity at 416 nm vs. 436 nm, is dependent on the TCPP concentration within the μM range (Table). There is a shift of the equilibrium towards the zwitterion at the highest concentration likely due to aggregation of the specie. In contrast to TSPP, ε at 650 nm is independent of concentration ($\varepsilon = 0.079$ and 0.076×10^5 M^{-1} cm^{-1} at 0.5 and 5 μM, respectively; n = 5; RSD = 1.1% and 6.8%, respectively). Acid-base titration of TCPP follows a different pattern than observed for TSPP (Section 2.4). With decreasing pH the absorbance at 416 nm initially decreases accompanied by an increase of the band at 436 nm (Fig. 4D). This band is broad, non-symmetrical and slightly red-shifted to 439 nm (FWHM = 75 nm, RSD = 3.6%, n = 5 at pH = 3.5), which suggests the presence of more than one absorbing species. In the pH range 1.2–5.0 the Soret band is severely flattened and broadened. As the expected pKa of the TCPP carboxylic groups is ∼ 4.2 (McMurry 2000), the absorption spectrum at pH 3–5 must be composed of several ionic species (Fig. 1), and possibly different aggregation states. pH titration does not result in a clear isosbestic point as expected for simple one-to-one transitions. At very low pH (< 2) the Soret band (416 nm) increases again (Fig. 4D) and gets more narrow (FWHM = 40 nm, RSD = 3.9%, n = 5 at pH = 1). This is caused by formation of the dication which is less likely to aggregate due to electrostatic intermolecular repulsion. The red Q-band is shifted to 661 nm and its absorptivity is increased. At alkaline pH TCPP exists in the free base form only (Fig. 1), resulting in a characteristic intense, narrow Soret band at 416 nm (FWHM = 15.5 nm at pH = 11.0, RSD = 0%, n = 5) and three Q-bands > 500 nm (Fig. 4D).

When TCPP is dissolved in methanol the band at 436 nm (i.e., zwitterion) is suppressed, likely as a result of a reduction of pKa-values similar to that observed for TSPP (Section 2.4). The four Q-bands are hypsochromically shifted (Table). The dependence of the absorbance at selected wavelength from methanol content is presented in Fig. 5G and 5I. Upon increasing the methanol content in aqueous mixtures ≥ 20% the absorbance at 416 nm increases linearly ($R^2 = 0.990$) up to 60% methanol content, parallel to a linear decrease at 436 nm ($R^2 = 0.988$), as also observed for TSPP (Section 2.4). However, there are no changes in the Soret band of TCPP at neither low (≤ 20%) nor high (≥ 60%) methanol content (Fig. 5G). There is also a linear decrease ($R^2 = 0.979$) of absorptivity at 650 nm at methanol content 0–40% (Fig. 5I), indicating a transition from zwitterion to free base. The absorbance at 416 nm is increased with a higher rate (slope + 0.043) than the parallel decrease at 436 nm

(slope –0.014). This can partly be ascribed to the presence of zwitterionic complexes of low absorptivity, which are gradually dissociated as the equilibrium switches towards the monomeric TCPP free base by addition of methanol.

TCPP seems to be solubilized by Tween® 80 micelles, as there is an apparent change in the absorption spectrum around cmc of the surfactant (Fig. 3B). At Tween® 80 concentrations below cmc the split Soret band is merged into one peak (FWHM = 60.5 nm, RSD = 2.9%, n = 5 at Tween® 80 concentration 0.0044 g/l) with lowered absorption and a shoulder at 403 nm, indicating the presence of several species. A band at 402 nm has previously been ascribed to formation of H-aggregates of TCPP in aqueous solution (Maiti et al. 1998). Above cmc the Soret band exhibits strong absorbance at 416 nm, and a further increase in surfactant concentration results in decreased absorption at 436 nm parallel to a linear increase ($R^2 = 0.986$) at 416 nm which is red shifted to 421 nm (Fig. 5H). The Q-band at 650 nm shows a nonlinear decrease with increasing concentration of Tween® 80, but no apparent wavelength shift (Table). The absorption spectrum above cmc is typical for porphyrin monomers, as characterized by one intense Soret band at 421 nm (FWHM = 14.5 nm, RSD = 2.4%, n = 5 at Tween® 80 concentration 1 g/l), four Q-bands, and concentration independent absorption (Table). The results indicate that Tween 80® below cmc forms premicellar complexes with TCPP. Above cmc, TCPP zwitterion aggregates are likely transformed into free base monomers due to reduced pKa_2 and solubilization.

A decrease in the absorption at 436 nm and at 650 nm upon addition of sodium chloride ($\mu = 0.05$ or 0.1 M) was observed but without any apparent increase in the corresponding peak at 416 nm (Table). An aqueous solution of 5 μM TCPP has its pH lowered from 6.4 in pure water to 5.9 at $\mu = 0.1$ M (n = 5, RSD = 0.3%), in accordance with the calculated decrease in pKa_2 by addition of NaCl (Fig. 1). As several species and aggregation states seem to be present at pH ~6, the exact effect of μ is hard to explain. At elevated temperature (37 °C) there is an increase in absorbance at 416 nm and a decrease at 436 nm at low TCPP concentration only (0.5 μM; Table). This is likely ascribed to temperature induced dissolution of zwitterionic dimers at low concentration, with a following shift of the equilibrium towards the free base, but may also involve a decrease in the pKa_2-value as observed for aromatic heterocyclic nitrogens (Ashton et al. 1982).

There was an apparent decrease in the absorbance at both 416 nm and 436 nm when the aqueous solution of TCPP was enriched with an equimolar concentration of ferric nitrate (Table) followed by a flattening and broadening of the Soret band (FWHM = 66.5 nm at 5 μM TCPP, RSD = 0.9%, n = 5), indicating the presence of coexisting species, which is reflected in the high RSD values at low TCPP concentration. The strong absorbance around 403 nm which is visible at 5 μM TCPP concentration suggests that TCPP forms aggregates in the presence of ferric ions, previously reported as H-aggregates (Maiti et al. 1998). As observed for TSPP, the use of tap water as a solvent removed the 436 nm band in the absorption spectrum of TCPP, the absorptivity at the Soret band was simultaneously increased and slightly shifted, and the Q-bands were shifted as compared to EMSURE® water (Table). A pharmaceutical formulation of TCPP will thus be highly dependent on the chemical purity of the excipients.

2.6. Inflection points and estimated pKa values

Porphyrins can exist in aqueous solution as differently charged species with various physicochemical properties. Determination of pKa values is therefore important in the evaluation of aggregation states and interactions between porphyrin and the vehicle. Previously published pKa-values differ, depending on the experimental design. Addition of sodium chloride influences the absorbance at the Soret band of TSPP and TCPP (Sections 2.4 and 2.5), counterions influence the aggregation pattern of TCPP (Choi et al. 2003), and addition of cosolvents modifies the pKa values (Farajtabar et al. 2010). For this reason it was decided to use simple and reproducible conditions, consisting of EMSURE® water at low ionic strength ($\mu = 0.1$ M) adjusted by NaCl for the determination of pKa values.

Acquisition of data during pH titration of the four porphyrins enabled pKa determination of the imino nitrogen atoms of TAPP, TSPP and TCPP, as described in Section 2.1, and the phenolic side groups of THPP. The same methodology as previously presented was applied (Lilletvedt et al. 2011), where the absorbance at the Soret band maximum was plotted against pH, and the inflection point (denoted pKa') was calculated by non-linear regression analysis. The Chi square values obtained when testing the goodness of fit varies (THPP: 0.16; TAPP: 0.53; TCPP: 0.81; TSPP: 0.44), which reflects the oversimplification of the proposed model. However the measured values fit well into the curve at the inflection points, as presented in Figs. 4A–D. As described in Section 2.1, the benzene substituents can be arranged according to their electron-withdrawing ability: $-N(Me)_3^+ > SO_3H >$ -COOH which correlates well with the inflection points (pKa') obtained for TAPP (3.6) < TSPP (4.6) < TCPP (6.0). This is consistent with a general rule that links a strong electron-withdrawing effect to increased acidity of organic molecules (McMurry 2000). The inflection point obtained for THPP (pKa' = 10.7) is close to pKa of phenol (pKa = 9.89; McMurry 2000), and probably represents the dissociation of the -OH substituents. Increased absorption in acidic environment (pH < 4.3) reflects increased solubility by protonation of the two imino nitrogen atoms of the THPP porphyrin core (Fig. 4A, inset). The estimated pKa_1-value ~ 4.5 for THPP was calculated by use of MarvinView software, Hungary. Experimentally determined inflection points were further corrected for the actual ionic strength ($\mu = 0.1$ M), in order to achieve the pKa values according to Sinko 2006. It yielded the following values: pKa = 2.3 (TAPP), pKa_2 = 10.8 (THPP), pKa_2 = 5.2 (TSPP), pKa_2 = 6.6 (TCPP).

Increase in the absorbance at the Soret band of TCPP at low pH ($pH \leq 2$; Fig. 4D, inset) reflects protonation of the carboxylic groups, with pKa-value ~ 4.2 (McMurry 2000), leading to subsequent monomerization. The calculated pKa_2 value of TSPP is in accordance with previous findings (pKa = 4.85, Farjtabar et al. 2010; pKa = 5.42, Kano 1996). The acidity constants of TCPP and TAPP have previously been investigated, but the methodology was not fully described (TAPP: pKa = 3.0; Kano et al. 1996) or the compound was only evaluated in silico (TCPP: pKa = 4.1 - 4.9; Kępczyński 2002). pH-titration of THPP has previously only been conducted in organic solvents or mixtures with water (Manna et al. 1995).

The porphyrin pKa-values will influence charge, aggregation, solubility, bioavailability, biological effect (photoreactivity) and adverse effects (e.g. anaphylactic reactions) of the photosensitizers, as well as physicochemical interactions with formulation excipients. Parenteral (e.g. for i.v. administration) or topical formulations of porphyrin photosensitizers developed for PDT of solid tumors or antimicrobial PDT will aim to monomerize, solubilize and stabilize the molecules *in vitro* and obtain drug targeting (e.g. by incorporation into nano particles) and improved bioavalability *in vivo*, in order to ensure or increase therapeutic effect. Various physicochemical properties of each photosensitizer (including the pKa-values) and a proper selection of excipients and formulation technology will be utilized in the further development of pharmaceutical PDT-formulations.

3. Experimental

3.1. Materials

5,10,15,20-Tetrakis(4-trimethylaniliniumphenyl) porphine tetrachloride (TAPP); 5,10,15,20-tetrakis(4-hydroxyphenyl) porphine (THPP); 5,10,15,20-tetrakis(4-sulphonatophenyl) porphine dihydrochloride (TSPP); 5,10,15,20-tetrakis(4-carboxyphenyl) porphine (TCPP), purity > 97%, were purchased from FrontierScientific, Logan, USA and used as received. The compounds were stored desiccated at + 4 °C. EMSURE® water (declared metal ion content, e.g. Cu ≤ 0.0004 mg/l, Fe ≤ 0.001 mg/l; p.a. grade) and Tween® 80 (Ph. Eur. quality) were purchased from Merck, Darmstadt, Germany. Purified water was obtained by distillation and ion exchange. Tap water has been taken from the laboratory, and used withour further purification. All other reagents were of p.a. quality.

3.2. Equipment

UV-visible absorption spectra (290–700 nm) were recorded using a Shimadzu UV-2401PC spectrophotometer. The computer software Kaleidagraph 4.0 (Synergy Software, US) was used for the nonlinear curve fitting. The computer software MarvinView 5.3.1 (ChemAxon, Budapest, Hungary) was used to calculate logD values and create 3-D molecular models. pH was measured by use of a pH 526 pH meter (WTW, Wellhelm, Germany), calibrated against pH-meter standards of pH 4.00; 7.00; and 10.00 (Merck, Darmstadt, Germany). A water bath M25 Lauda produced by Houm AS, Grefsen, Norway, was used for temperature equilibration (37 ± 0.1 °C).

3.3. Methods

3.3.1. UV-visible absorption measurements and preparation of samples

UV-visible absorption spectra of THPP; TAPP; TCPP; and TSPP (0.5 μM and 5 μM) were recorded in various vehicles, in order to determine pKa-values and to evaluate the influence of medium properties and excipients on absorption properties and the process of aggregation for each compound. The accuracy in wavelength determination of the instrumentation was ± 0.5 nm. Samples were wrapped in aluminum foil prior to use in order to protect from light exposure. Experiments were conducted at ambient temperature and by use of Emsure® water, unless stated otherwise. A stock solution of each of the porphyrins was prepared in methanol at 0.025–0.25 mM. The methanol concentration in in the aqueous solutions never exceeded 2% (v/v) of the sample. A solution of Tween® 80 in Emsure® water (2.5 g/l) was prepared and left overnight in the refrigerator, in order to remove the foam before use. All stock solutions were stored at + 4 °C for maximum 4 days.

3.3.2. Influence of methanol-water mixtures

Absorption spectra of the four *meso*-porphyrins were recorded in methanol:Emsure® water mixtures at 0%, 5%, 10%, 20%, 30%, 40%, 50%, 60%, 70%, 80%, 90% and 100% methanol (n = 3). The absorbance at selected wavelengths was plotted against methanol concentration in order to evaluate the influence of the medium on aggregation and solubility of the selected compounds.

3.3.3. Influence of Tween® 80

Absorption spectra of the four *meso*-porphyrins were recorded in Tween® 80:Emsure® water, 0.00004% - 0.4% (w/v) (n ≥ 5). Absorbance at selected wavelengths was plotted against the Tween® 80 concentration, in order to evaluate the influence of surfactant concentration on aggregation and solubility of the selected compounds.

3.3.4. Influence of temperature and water quality

Absorption spectra of the four *meso*-porphyrins were recorded in tap water, purified water and Emsure® water; at room temperature and at 37 ± 0.1 °C (n = 5), in order to determine the influence of water quality and temperature on the absorption properties. For measurements at elevated temperature both the laboratory glassware and the solvents were pre-heated to 37 °C, and every measurement was done within few minutes sample preparation. However, the used spectrophotometer did not have a temperature control system.

3.3.5. Influence of ionic strength and ferric ions

Absorption properties of the four *meso*-porphyrins were analyzed in 0.05 M and 0.1 M aqueous solutions of NaCl (n = 5); and in 5 μM and 0.5 μM solutions of $Fe(NO_3)_3 \times 9\ H_2O$. The purpose was to evaluate the influence of ionic strength and ferric ions on the absorption properties of the selected porphyrins.

3.3.6. Determination of inflection points (pKa') and estimation of pKa-values

Absorption spectra of the four *meso*-porphyrins (5 μM) were recorded as a function of pH in the range 1–13 at ambient temperature immediately after sample preparation (n = 3), in order to determine the inflection points (pKa') and estimate the pKa-values of the compounds. Changes in the molar absorptivity of the Soret band at selected wavelengths due to pH variations were used in the calculation of the inflection points by nonlinear regression analysis. The computer software Kaleidagraph 4.0 (Synergy Software, US) was used for the curve fitting. Aqueous solutions of 0.1 M NaOH and 0.1 M HCl were used to modulate the pH. The ionic strength was kept constant (μ = 0.1 M) by addition of NaCl (0.1 M), and taken into account in the calculation of the pKa-values.

Acknowledgements: This work was kindly supported by the Norwegian Research Council.

References

Ashton LA, Bullock JI, Simpson PWG (1982) Effect of temperature on the protonation constants of some aromatic, heterocyclic nitrogen bases and the anion of 8-hydroxyquinoline. J Chem Soc Faraday Trans 78: 1961–1970.

Choi MY, Pollard JA, Webb MA, McHalle JL (2003) Counterion-dependent excitonic spectra of tetra(p-carboxyphenyl) porphyrin aggregates in acidic aqueous solution. J Am Chem Soc 125: 810–820.

Cormick MP, Alvarez MG, Rovera M, Durantini EN (2009) Photodynamic inactivation of Candida albicans sensitized by tri- and tetra-cationic porphyrin derivatives. Eur J Med Chem 44: 1592–1599.

Corsini A, Herrmann O (1986) Aggregation of meso-tetra-(p-sulphonatophenyl) porphine and its Cu(II) and Zn (II) complexes in aqeous solution. Talanta 33: 335–339.

Cunderlikova B, Bjørklund EG, Pettersen EO, Moan J (2001) pH-dependent spectral properties of HpIX, TPPS2a, mTHPP and mTHPC. Photochem Photobiol 74: 246–252.

Eszter-Borbas K, Lahaye D (2008) Photodynamic therapy of Cancer. In: Missailidis S (ed.) Anticancer Therapeutics, John Wiley & Sons Ltd., Chichester, pp. 187–223.

Farajtabar A, Gharib F (2010) Solvent effect on protonation constants of 5,10,15,20-tetrakis(4-sulfonatophenyl) porphyrin in different aqueous solutions of methanol and ethanol. J Sol Chem 39: 231–244.

Gouterman M (1978) Optical spectra and electronic structure of porphyrins and related rings, In: Dolphin D. (ed.) Porphyrins, Volume III, Academic Press, New York, pp. 1–165.

Guthrie JP (1978) Hydrolysis of esters of oxy acids: pKa values for strong acids; Brønsted relationship for attack of water at methyl; free energies of hydrolysis of esters of oxy acids; and a linear relationship between free energy of hydrolysis and pKa holding over a range of 20 pK units. Can J Chem 56: 2342–2354.

Hamblin MR, Miller JL, Rizvi I, Loew HG, Hasan T (2003) Pegylation of charged polymer-photosensitiser conjugates: effects on photodynamic efficacy. Brit J Cancer 89: 937–943.

Janson TR, Katz JJ (1972) Examination of 220 Mhz NMR-spectra of mesoporphyrin-IX-dimethylesther, deuteroporphyrin-IX dimethylester and protoporphyrin-IX dimethylester. J Magn Reson 6: 209–220.

Kadish KM, Maiya GB, Araullo C, Guillard R (1989) Micellar effects on the aggregation of tetraanionic porphyrins. Spectroscopic characterization of free-base meso-tetrakis(4-sulfonatophenyl)porphyrin, $(TPPS)H_2$, and (TPPS)M (M = Zn(II), Cu(II), $V0^{2+}$) in aqueous micellar media. Inorg Chem 28: 2125–2131.

Kano K, Takei M, Hashimoto S (1990) Cationic porphyrins in water. ^1H NMR and fluorescence studies on dimer and molecular complex formation. J Phys Chem 94: 181–187.

Kano K, Tanaka N, Minamizono H, Kawakita Y (1996) Tetraarylporphyrins as probes for studying mechanism of inclusion-complex formation of cyclodextrins. Effect of microscopic environment on inclusion of ionic guests. Chem Lett 25: 925–926.

Kępczyński M, Pandian RP, Smith KM, Ehrenberg B (2002) Do liposome-binding constants of porphyrins correlate with their measured and predicted partitioning between octanol and water? Photoch Photobiol 76: 127–134.

Li X, Li D, Zeng W, Zou G, Chen Z (2007) Tuning J-aggregates of tetra(p-hydroxyphenyl)porphyrin by the headgroups of ionic surfactants in acidic nonionic micellar solution. J Phys Chem B 111: 4342–4348.

Lilletvedt M, Tønnesen HH, Høgset A, Sande SA, Kristensen S (2011) Evaluation of physicochemical properties and aggregation of the photosensitizers TPCS2a and TPPS2a in aqueous media. Pharmazie 66: 325–333.

Ma H-L, Jin W-J (2008) Studies on the effects of metal ions and counter anions on the aggregate behaviors of meso-tetrakis(p-sulfonatophenyl) porphyrin by absorption and fluorescence spectroscopy. Spectrochim Acta Part A 71: 153–160.

Maiti NC, Ravikanth M, Mazumdar S, Periasamy N (1995) Fluorescence dynamics of noncovalently linked porphyrin dimers and aggregates. J Phys Chem 99: 17192–17197.

Maiti NC, Mazumdar S, Periasamy N (1998) J- and H-aggregates of porphyrin-surfactant complexes: time-resolved fluorescence and other spectroscopic studies. J Phys Chem B 102: 1528–1538.

Manna BK, Bera SC, Rohatgi-Mukherjee KK (1995) Effect of solvent and pH on the spectral characteristics of mesotetrakis(p-hydroxyphenyl) porphyrin in dimethylformamide and dimethylformamide + water mixed solvents. Spectrochim Acta 51: 1051–1060.

McMurry (2000) In: Organic Chemistry, 5th edition, Brooks/Cole, Pacific Grove, pp. 607, 821, 824, 660.

Mojzisova H, Bonneau S, Brault D (2007) Structural and physico-chemical determinants of the interactions of macrocyclic photosensitizers with cells. Eur Biophys J 36: 943–953.

Moreira LM, dos Santos FV, Lyon JP, Maftoum-Costa M, Pacheco-Soares C, da Silva NS (2008) Photodynamic therapy: porphyrins and phthalocyanines as photosensitizers. Aust J Chem 61: 741–754.

Oba T (2007) Photosensitizer nanoparticles for photodynamic therapy. Curr Bioact Comp 3: 239–251.

O'Connor AE, Gallagher WM, Byrne AT (2009) Porphyrin and nonporphyrin photosensitizers in oncology: preclinical and clinical advances in photodynamic therapy. Photochem Photobiol 85: 1053–1074.

Ohno O, Kaizu Y, Kobayashi H (1993) J-aggregate formation of a water-soluble porphyrin in acidic aqueous media. J Chem Phys 99: 4128–4139.

Papkovskii DB, Savitskii AP, Ponomarev GV (1989) Fluorescence of porphyrins in aquous solutions of surfactants. J Appl Spectr 51: 786–790.

Pasternack RF, Huber PR, Boyd P, Engasser G, Francesconi L, Gibbs E, Fasella P, Venturo GC, de Hinds L (1972) On the aggregation of meso-substituted water-soluble porphyrins. J Am Chem Soc 94: 4511–4517.

Phillips JN (1960) The ionization and coordination behaviour of porphyrins. Rev Pure Appl Chem 10: 35–59.

Seidlitz HK, Schneckenburger H, Stettmaier K (1990) Time-resolved polarization measurements of porphyrin fluorescence in solution and in single cells. J Photochem Photobiol B 5: 391–400.

Sinko PJ (2006) Ionic equilibria. In: Troy D (ed.) Martin's physical pharmacy and pharmaceutical sciences, 5th edition, Lippincott Williams & Wilkins, Baltimore, p. 181.

Thompson AN, Krishnamurthy M (1979) Peripheral charge effect on the kinetics of Zn (II)-porphyrin system. J Inorg Nucl Chem 41: 1251–1255.

Torchilin VP (2007) Micellar nanocarriers: pharmaceutical perspectives. Pharm Res 24: 1–16.

Wan LSC, Lee PFS (1974) CMC of polysorbates. J Pharm Sci 63: 136–137.